Electronic Supplementary Material (ESI) for Nanoscale.
This journal is © The Royal Society of Chemistry 2020

Supporting Information

Amorphous TiO_2 as Multifunctional Interlayer Boosting Efficiency and Stability of CdS-Cobaloxime Hybrid System for Photocatalytic Hydrogen Production

Hongkai Zhao[a,b], Xiaoxia Li[c], Mingyue Zheng[b], Xian Zhao[b], Qun Zhang*[c], Yi Luo[c], Weiliu Fan*[a]

[a] School of Chemistry and Chemical Engineering, Shandong University, Jinan, 250100, China

[b] Institute of Crystal Materials and State Key Laboratory of Crystal Materials, Shandong University, Jinan, 250100, China

[c] Hefei National Laboratory for Physical Sciences at the Microscale, University of Science and Technology of China, Hefei, Anhui, 230026, China

Computational details and models

All DFT (density functional theory) calculation were performed by using code from the Vienna Ab initio Simulation Package (VASP).[1] A projector augmented-wave method was used to describe the core electrons. The exchange correlation potential was described using the Perdew-Burke-Ernzerhof (PBE) functional within the generalized gradient approximation (GGA).[2] The energy cutoff of the plane-wave basis set was chosen to be 450 eV. The Monkhorst–Pack scheme k-point grids were set: 2×2×1 for the a-TiO_2 ,6×6×6 for the CdS bulk, and 2×2×1 for the CdS (110) surface. The convergence criterion for the total energy was set to 1×10^{-4} eV, and that of the force on each atom was set to 0.02 eV/Å. Spin-polarized calculations were performed.

The structures of CdS(110) surface and the amorphous TiO_2 (a-TiO_2) are illustrated in Fig. S1. The amorphous TiO_2 phase was modeled using 120-atom supercell of size about 11×11×11 Å^3. The sample obtained from MD were further relaxed to achieve the ground state configuration using DFT computations before calculating.[3] The CdS(110) surface lattice vectors were 13.7 Å and 14.5 Å to give a 3 ×4 supercell. Each supercell had ~20 Å vacuum between them to avoid self-interaction effects of periodic boundary conditions. In the calculation process, the bottom three atoms are fixed and the remaining atoms are relaxed.

In this paper, the corresponding adsorption energy of the molecule were obtained by the following equation:

$$E_{ads} = E_{cat+mol} - E_{cat} - E_{mol}$$

where $E_{cat+mol}$ is the total energy of the system after molecular adsorption, E_{cat} is the energy of the catalyst only, and the E_{mol} is the energy of the molecule.

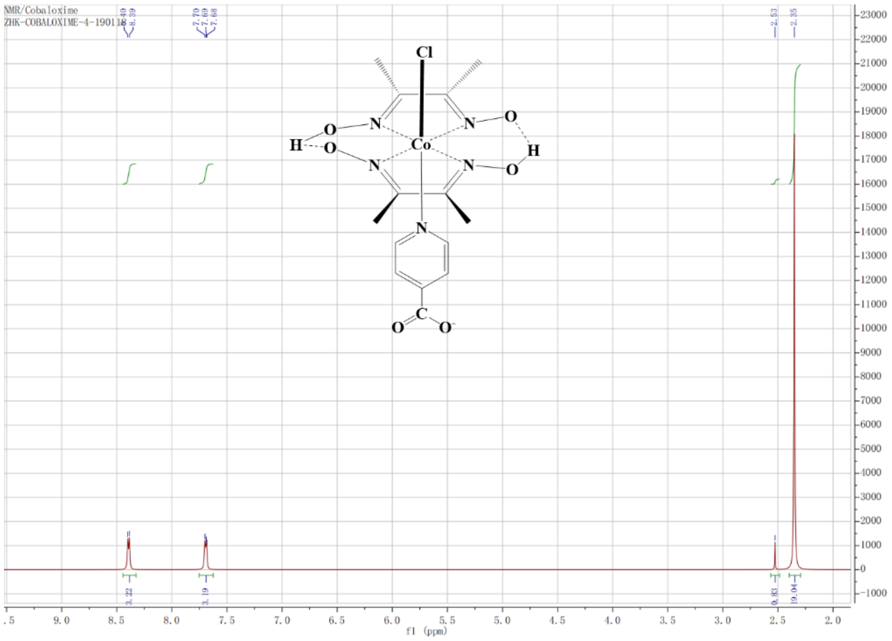

Fig. S1. NMR spectrum of (HOOCpy)Co(dmgH)$_2$(Cl).

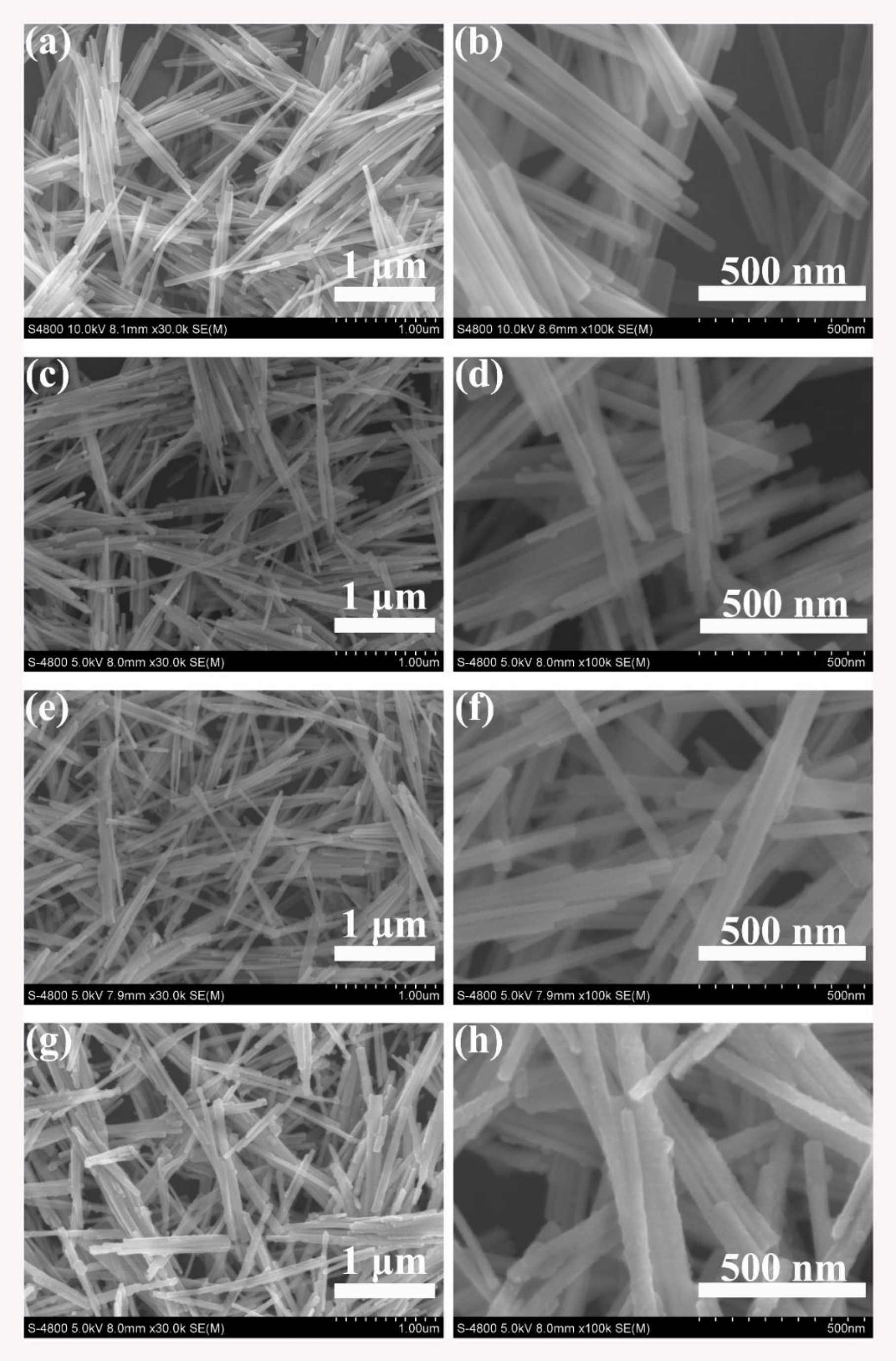

Fig. S2. SEM of CdS (a, b), CT-1 (c, d), CT-2 (e, f) and CT-3 (g, h).

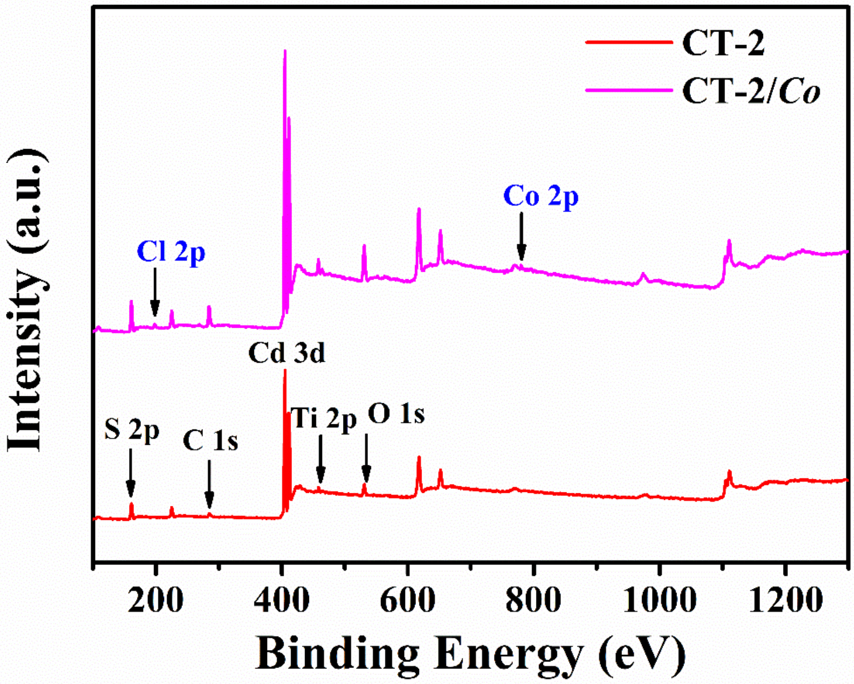

Fig. S3. XPS survey spectrum of CT-2 and CT-2/***Co***.

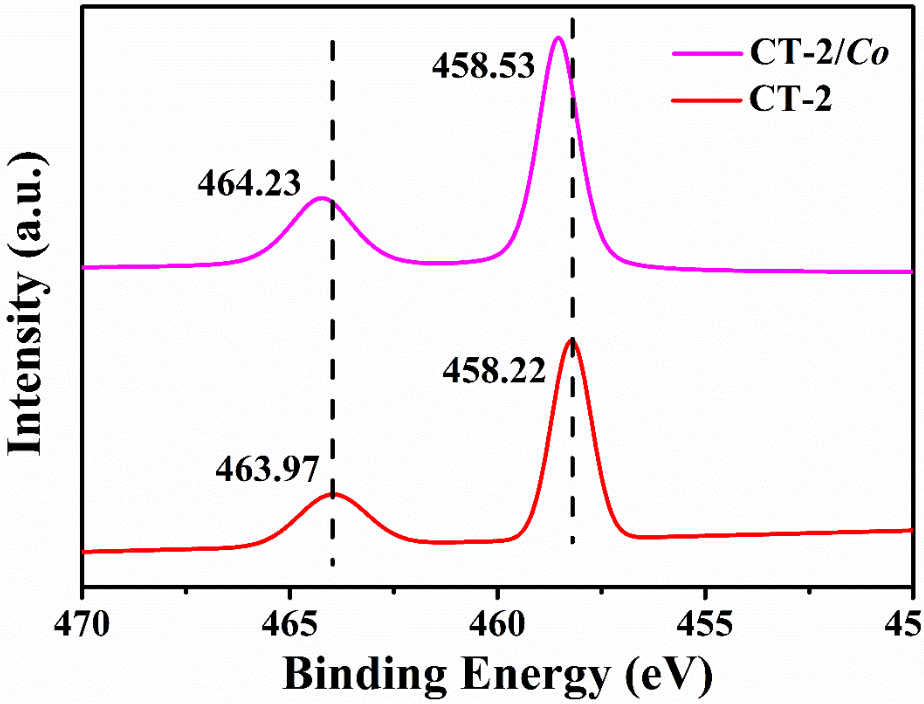

Fig. S4. XPS spectra of Ti 2p peaks of CT-2 and CT-2/*Co*.

XPS is an effective method to characterize interfacial bonding between semiconductors and molecules.[4] The fitting peak of Ti $2p_{1/2}$ and Ti $2p_{3/2}$ for CT-2 and CT-2/***Co*** were located at binding energies of 458.22, 463.97 eV and 458.53, 464.23 eV, respectively, as seen in **Fig. S4**, CT-2/***Co*** is shifted 0.31 eV for Ti 2p$_{1/2}$ and 0.26 eV for Ti 2p$_{3/2}$ in comparison to the peaks in CT-2 samples. The Ti 2p binding energies for CT-2/***Co*** increased due to the decrease in the electron density, which indicates that the strong coordination bond between carboxyl groups of molecular ***Co*** and Ti atoms of CT-2.

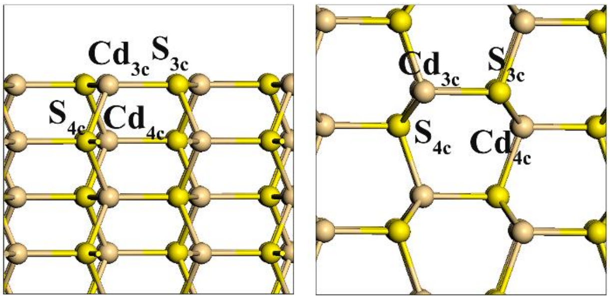

CdS(110)

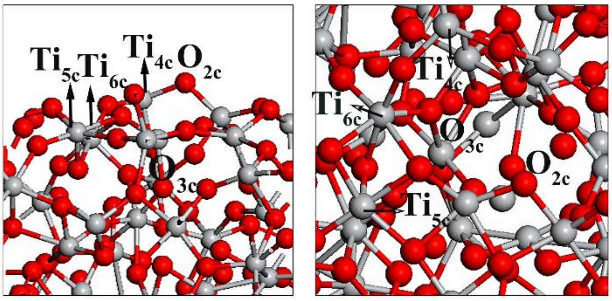

a-TiO$_2$

Fig. S5. Side view and top view of CdS(110) surface the a-TiO$_2$. The yellow, fleshcolor, light gray, dark gray, red, blue and white balls represent Cd, S, C, Ti, O, N and H atoms, respectively.

The surface configurations of the CdS (110) and a-TiO$_2$

The configurations of the CdS(110) surface and a-TiO$_2$ used in our calculations are shown in Fig. S5. The outermost atoms of the regular CdS(110) surface are threefold coordinated cadmium (Cd$_{3c}$), fourfold coordinated cadmium (Cd$_{4c}$) ,threefold coordinated sulfur (S$_{3c}$), and fourfold coordinated sulfur (S$_{4c}$)). The crystalline (anatase) TiO$_2$ surface contains fivefold coordinated titanium (Ti$_{5c}$), sixfold coordinated titanium (Ti$_{6c}$), twofold coordinated oxygen (O$_{2c}$), and threefold coordinated oxygen (O$_{3c}$). While there is also fourfold coordinated titanium (Ti$_{4c}$) on amorphous TiO$_2$ (a-TiO$_2$), which is the low coordinate number of surface titanium atom. In the experiments, we also found coordination unsaturated Ti atoms in a-TiO$_2$. (XPS spectra in Fig. S13)

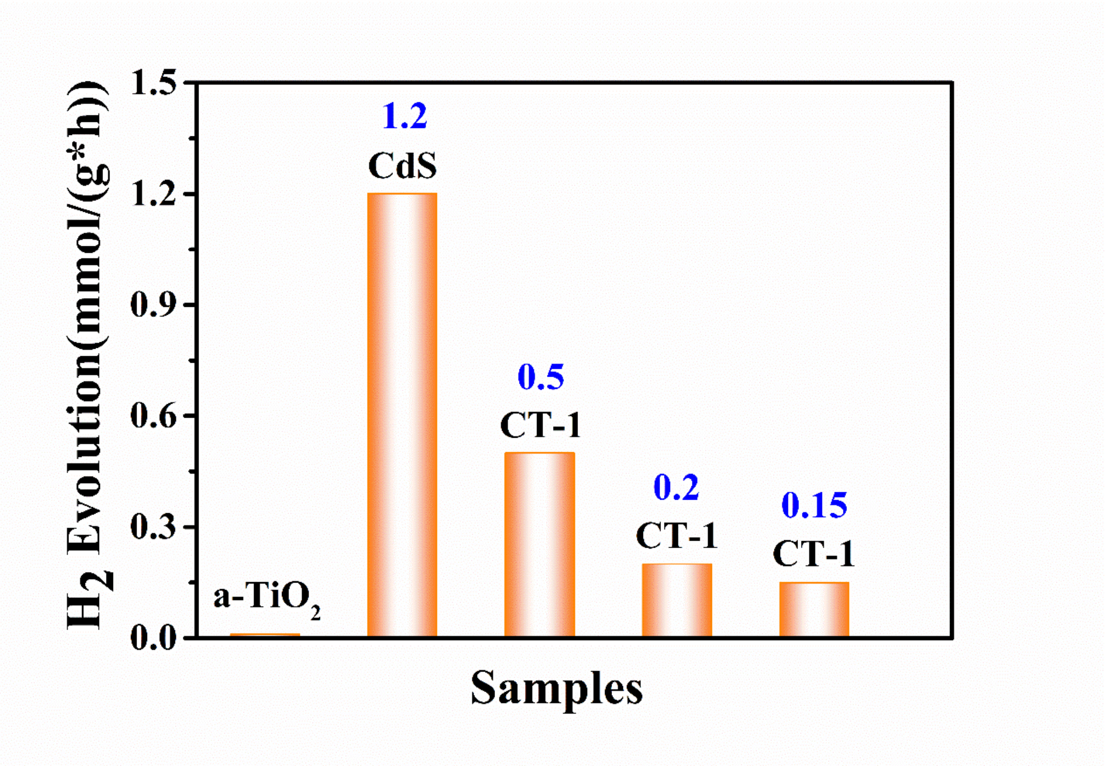

Fig. S6. Photocatalytic H_2 production rates of samples a-TiO_2, CdS, CT-1, CT-2 and CT-3 under visible light (λ ≥ 420 nm). Photocatalytic reaction solution including 10 mg photocatalyst, 10 mL lactic acid in 90 mL ultrapure water.

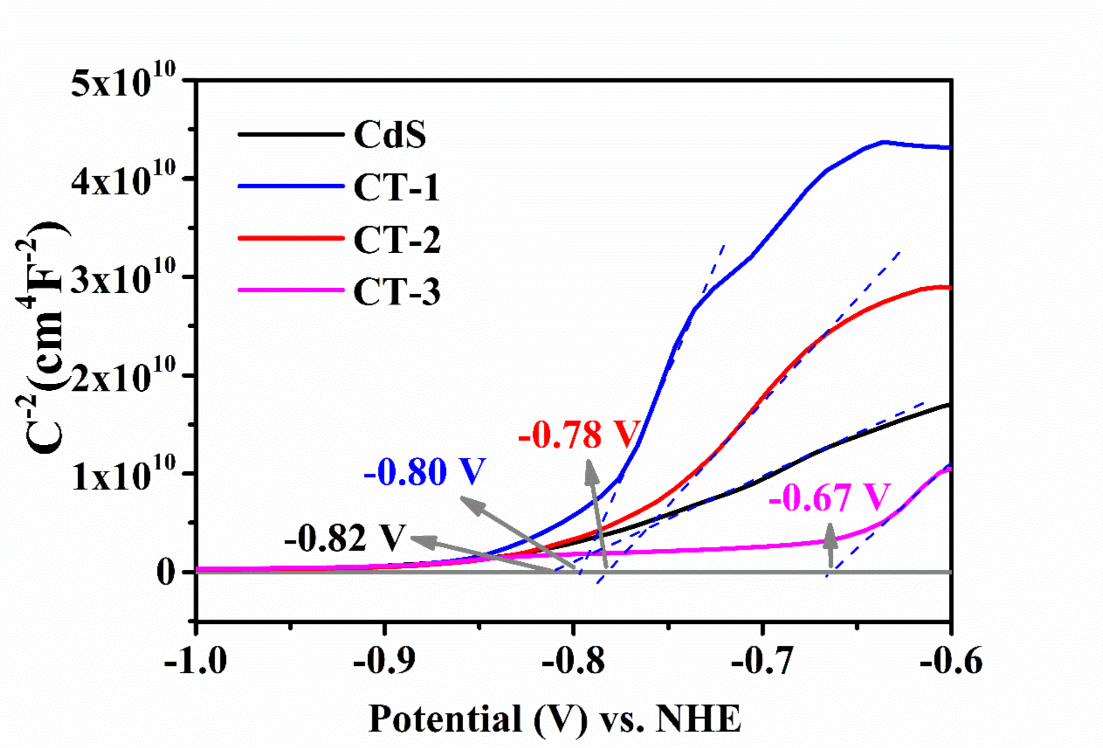

Fig. S7. Mott-Schottky plots of CdS and CT electrodes obtained in 0.5 M Na_2SO_4 aqueous solutions containing 10 mL LA.

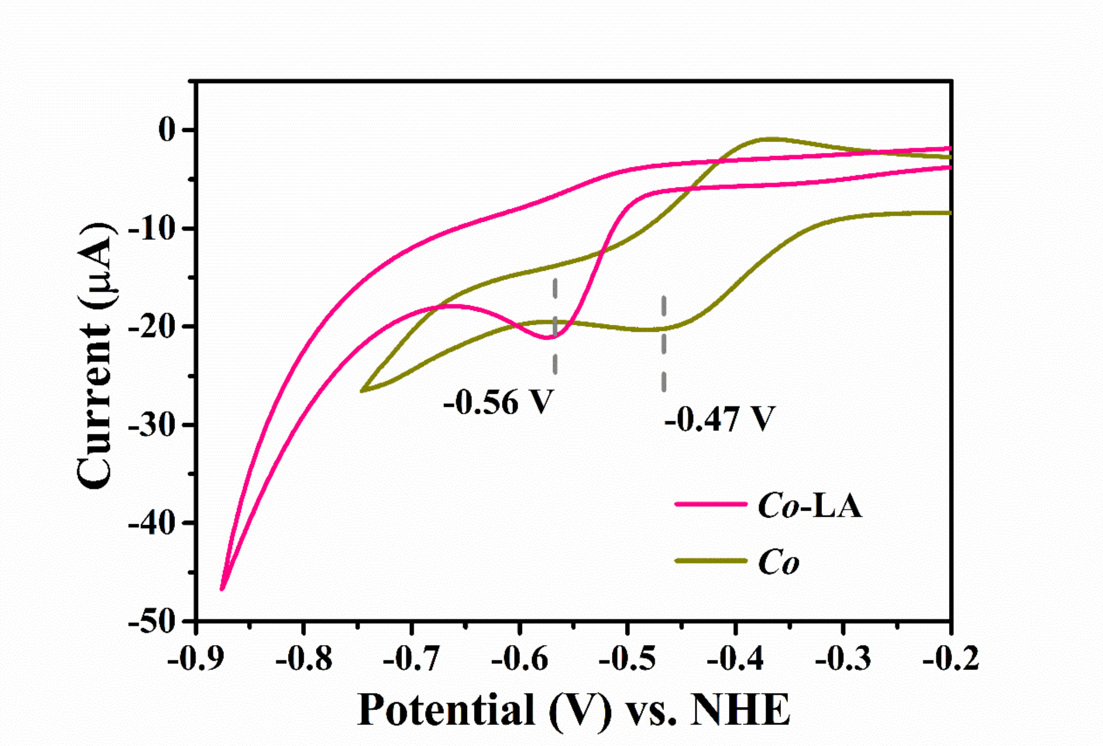

Fig. S8. The CVs of ***Co*** measured at 0.5 M Na_2SO_4 aqueous solutions with 0.25 mM concentration ***Co*** and 10 mL LA.

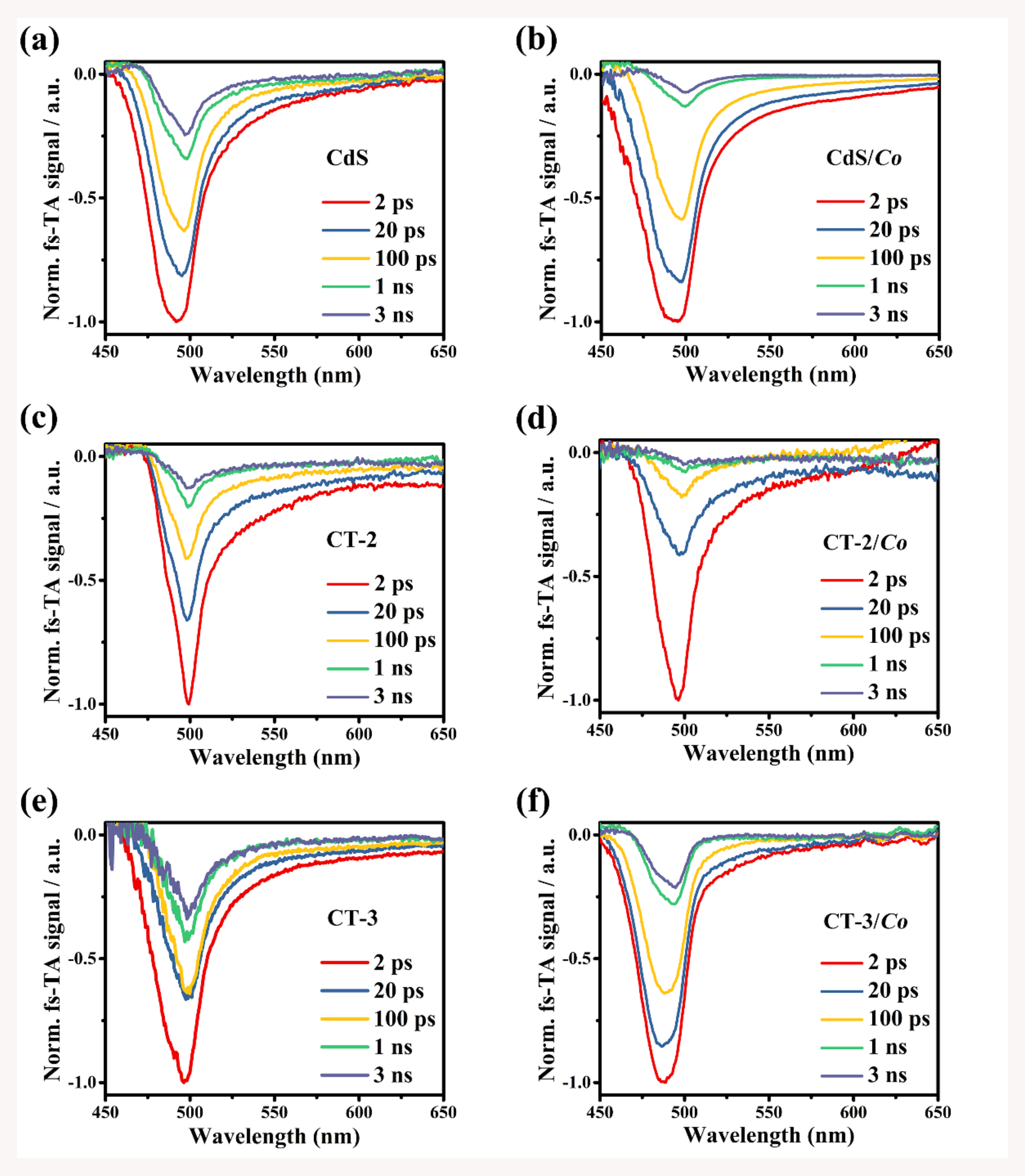

Fig. S9. Transient absorption spectra of (a) CdS NRs, (c) CT-2, (e) CT-3 and corresponding samples decorated with molecular ***Co*** (b) CdS/***Co***, (d) CT-2/***Co***, (f) CT-3/***Co*** taken at several indicated probe delay times (pump at 400 nm).

Table S1. Relaxation Time Constants for the Investigated Systems[a]

System	τ_1/ps	τ_2/ps	τ_3/ps	τ_{av} /ps
CdS	14.7±0. (24%)	177±4 (43%)	2326±85 (33%)	2126 ± 80
CdS-Co	9.3±0.5 (44%)	106±8 (32%)	1781±167 (24%)	1642±156
CT-2	4.0±0.8 (11%)	166±5 (73%)	1440±193 (16%)	1007 ±188
CT-2-Co	0.9±0.1 (49%)	12.3±0.3 (38%)	265±11 (13%)	231 ±9
CT-3	6.4±0.5 (43%)	71±11 (18%)	1832±120 (39%)	1795 ±104
CT-3-Co	3.6±0.3 (17%)	131±2 (54%)	1564±53 (29%)	1366 ±50

[a] The corresponding statistical weights from the triexponential fitting are given in the parentheses.

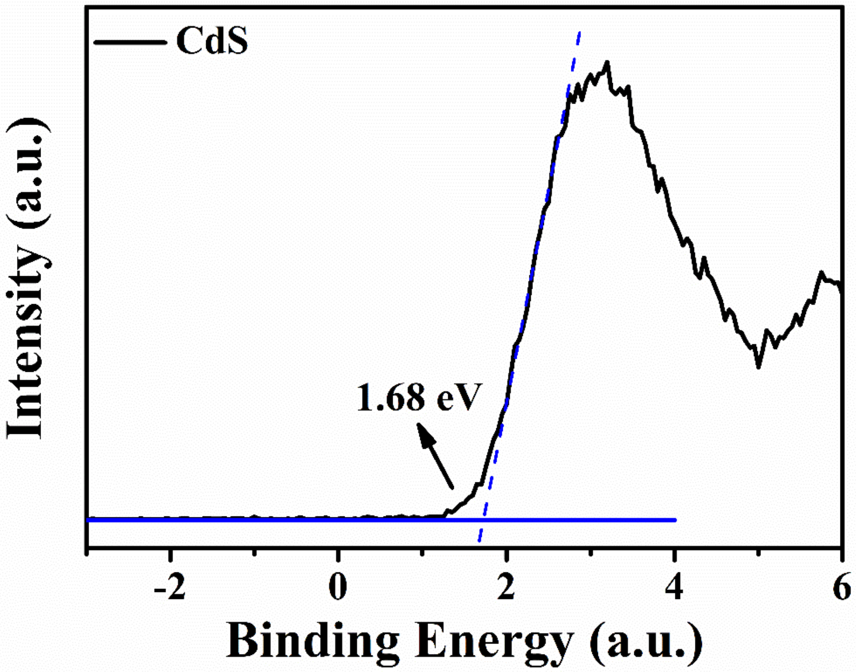

Fig. S10. X-ray photoemission valence spectrum of pure CdS NRs.

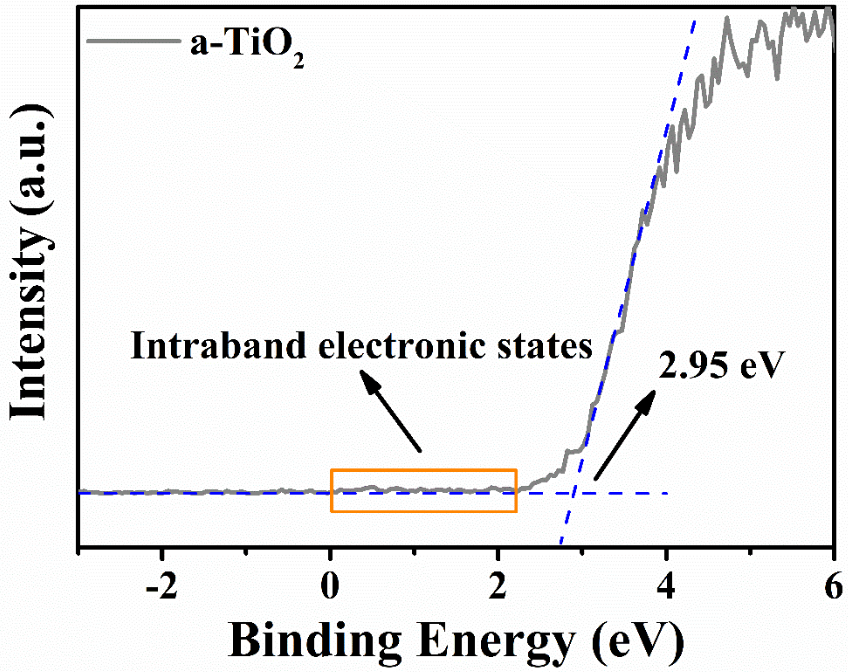

Fig. S11. X-ray photoemission valence spectrum of amorphous TiO_2.

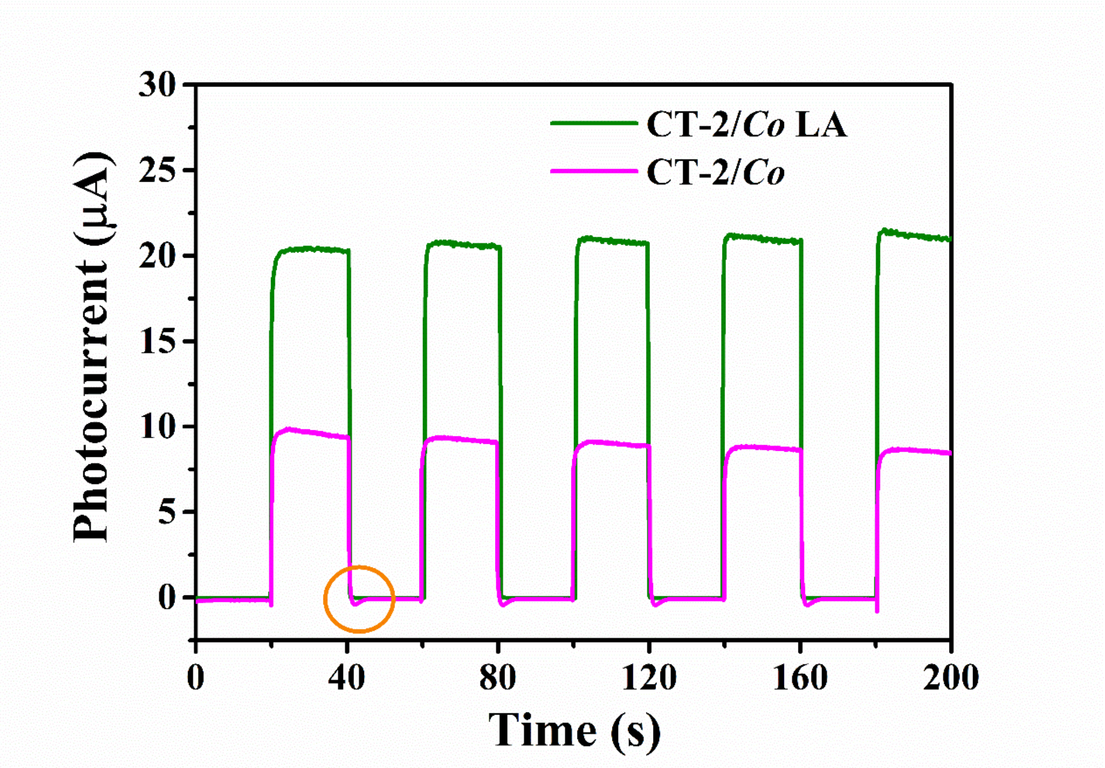

Fig. S12. Transient photocurrent response of CT-2/***Co*** electrode in 0.5 M Na_2SO_4 solution with LA and without LA under visible light irradiation (λ > 420 nm).

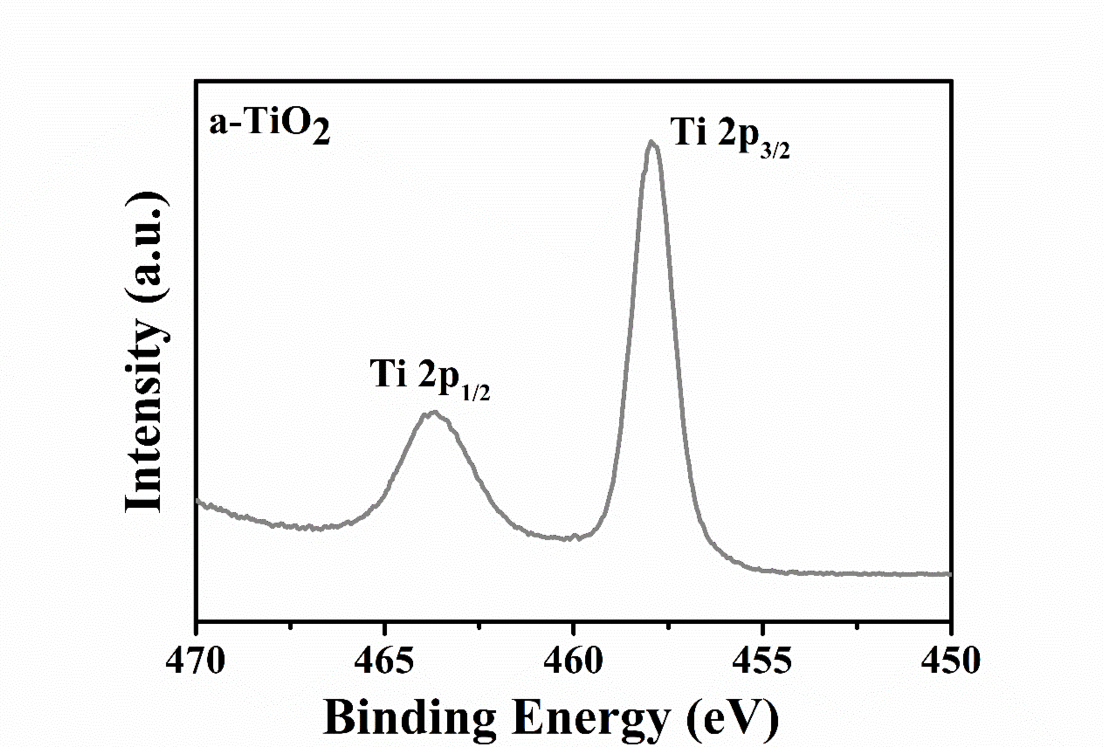

Fig. S13. XPS spectra of Ti 2p. The binding energy of Ti $2p_{3/2}$ and Ti $2p_{1/2}$ are located at 464.3 and 458.6 eV, respectively, posting between Ti^{4+} and Ti^{3+}.[5]

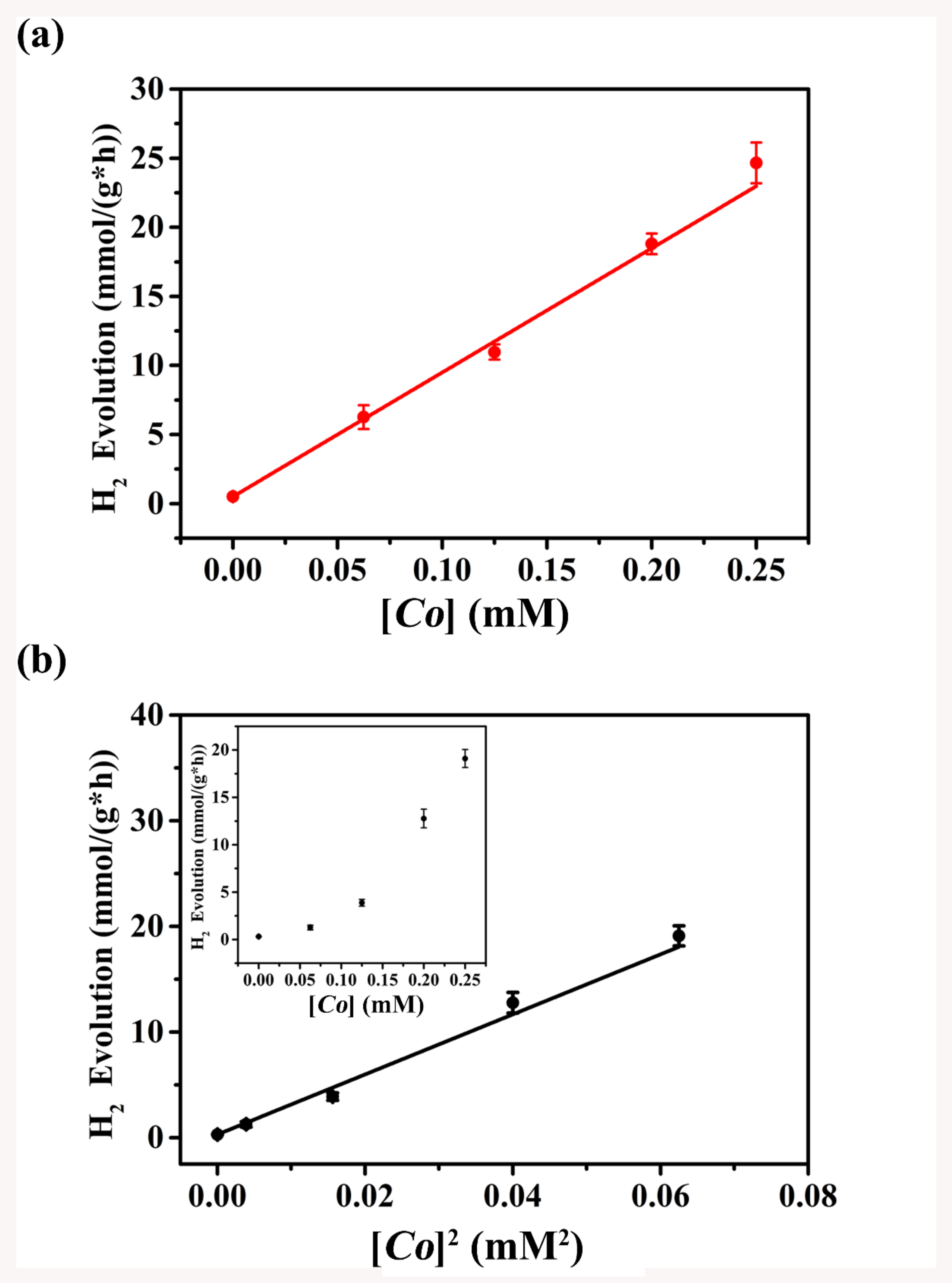

Fig. S14. (a) Initial H_2 evolution rate of CT-2/***Co*** as a function of [***Co***]. (b) Initial H_2 evolution rate of CdS/***Co*** as a function of [***Co***]^2 (inset: initial H_2 evolution rates as a function of [***Co***]). Photocatalytic H_2 evolution reaction of all samples were test for 3h.

In the photocatalytic process of semiconductor-molecular catalysts hybrid systems, the corresponding molecular catalyst concentration also has an equilibrium value, when the amount of semiconductor is fixed, the amount of hydrogen produced does not necessarily increase with the amount of molecular catalyst as originally stated. In order to verify the possible catalytic pathway of the two hybrid systems in, we selected a concentration of ***Co*** range between 0 and 0.25 mM. In general, the concentration of the molecular catalyst is lower than 0.25 mM for testing. The results in Fig. S14 clearly show hydrogen production has a linearization dependence on [***Co***]^2 in CdS/***Co*** hybrid system which implies a homolytic pathway, while has a linearization dependence on [***Co***] in CT-2/***Co*** hybrid system which implies a heterolytic pathway.

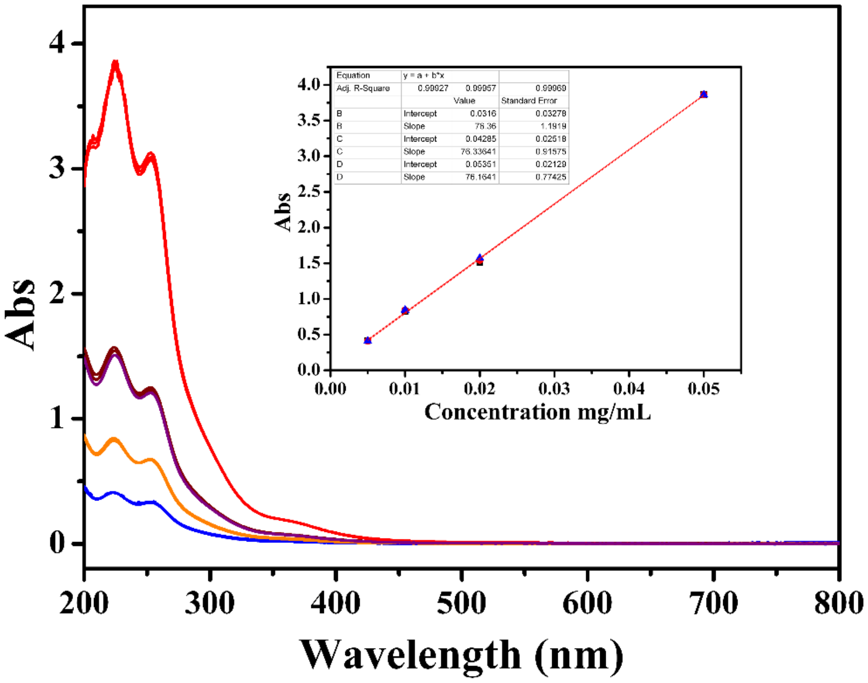

Fig. S15. UV-Vis spectra of different ***Co*** solution and the corresponding standard curve.

Reference

[1] Kresse, G.; Furthmüller, J. Efficient Iterative Schemes for ab Initio Total-Energy Calculations Using a Plane-Wave Basis Set. *Phys. Rev. B* **1996**, *54*, 11169−11186.

[2] Perdew, J. P.; Burke, K.; Ernzerhof, M. Generalized Gradient Approximation Made Simple. *Phys. Rev. Lett.* **1996**, *77*, 3865−3868.

[3] Kulbir Kaur Ghuman, Chandra Veer Singh. Effect of doping on electronic structure and photocatalytic behavior of amorphous TiO_2. J. Phys.: Condens. Matter 25 (2013) 475501 (11pp).

[4] Liu, G.; Jaegermann, W.; He, J.; Sundström, V.; Sun, L. XPS and UPS Characterization of the TiO_2/ZnPcGly Heterointerface: Alignment of Energy Levels. *J. Phys. Chem. B* **2002**, *106* (23), 5814–5819. https://doi.org/10.1021/jp014192b.

[5] H. Zhou and Y. R. Zhang, *J. Phys. Chem. C.*, 2014, **118**, 5626-5636